J. Membrane Biol. 53, 19–32 (1980)

The Journal of
Membrane Biology

Occluding Junctions in a Cultured Transporting Epithelium: Structural and Functional Heterogeneity

Marcelino Cereijido, Enrique Stefani, and Adolfo Martínez Palomo

Departments of Physiology and Cell Biology, Centro de Investigación y de Estudios Avanzados del I.P.N., México 14, D.F., México

Summary. MDCK cells (epithelioid of renal origin) form monolayers which are structurally and functionally similar to transporting epithelia. One of these similarities is the ability to form occluding junctions and act as permeability barriers. This article studies the junctions of MDCK monolayers formed on a permeable and transparent support (a disk of nylon cloth coated with collagen) by combining two different approaches: (i) *Scanning of the electric field:* the disk is mounted as a flat sheet between two Lucite chambers and pulses of 20–50 μA cm^{-2} are passed across. The apical surface of the monolayer is then scanned with a microelectrode to detect those points where the current is flowing. This shows that the occluding junctions of this preparation are not homogeneous, but contain long segments of high resistance, intercalated with sites of high conductance. (ii) *Freeze fracture electron microscopy:* the junctions are composed of regions of eight to ten strands intercalated with others where the strands are reduced to one or two ridges. The sites of high conductance may correspond to those segments where the number of junctional strands is reduced to 1 or 2. It is concluded that the occluding junctions of MDCK monolayers are functionally and morphologically heterogeneous, with "tight" regions intermixed with "leaky" ones.

Cultures of the MDCK cell line (Madin & Darby, 1958) form *in vitro* cell monolayers with functional properties analogous to those of transporting epithelia (Misfeldt, Hammamoto & Pitelka, 1976; Cereijido et al., 1978*a* and *b*). (For a recent review, *see* Handler, Perkins & Johnson, 1979.) These properties arise from the structural and functional polarity of MDCK plasma membrane, studied in a previous article (Cereijido et al., 1979), and from the ability of MDCK cells to make occluding junctions which control the permeability through the paracellular route. In the present study we investigate the structure and functional properties of the junctional complexes of MDCK monolayers by means of electron microscopy and a new electric field scanning method of high spatial resolution.

Monolayers of MDCK cells prepared on a permeable and transparent support (a disk of a nylon cloth coated with collagen) can be mounted, as a flat sheet between two Lucite chambers for membrane transport studies. At the passage of cells used ($100–110^{th}$), these monolayers show an electrical resistance of 70–200 Ωcm^2. Therefore, the monolayer can be compared to the so-called leaky epithelia. Yet, the concept of epithelial leakiness derives from the permeability of the paracellular conductive pathway and might not be necessarily related to the macroscopic transmural electrical resistance. Thus, Augustus, Bijaman, van Os and Slegers (1977) have shown that the salivary gland ductal epithelium has a very low electrical resistance due to a high Cl-conductance, yet the paracellular pathways of the epithelium are very tight. Therefore, in order to assess the permeability of the paracellular route in MDCK monolayers, a parameter that depends directly on the degree of tightness of the occluding junctions, we resorted to two different experimental approaches: (i) We have passed small pulses of current through the monolayer and scanned with a microelectrode moved along the apical surface of the cells, looking for conductive spots. This procedure has some similarities with the one used by Frömter and Diamond (1972) and Frömter (1972); however, we have used pulses about two orders of magnitude smaller in intensity, and two orders of magnitude shorter in time, with a minimal microelectrode separation (8 μm), which allow a fine discrimination between conducting and nonconducting sites. (ii) Freeze-fracture electron microscopy was applied to study the distribution of the junctional strands along the occluding junctions.

0022-2631/80/0053-0019 $02.80

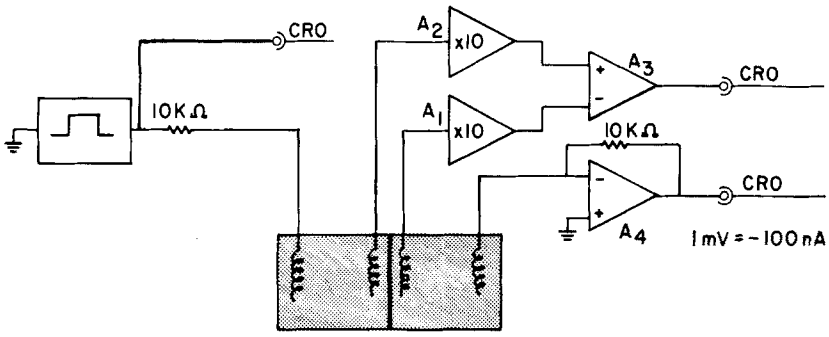

Fig. 1. Electrical diagram for total membrane resistance and capacity measurements. The disk containing the monolayer was mounted as a flat sheet between two Lucite chambers containing MEM. Voltage drop across the membrane was recorded via A_1 and A_2 amplifiers and differentially substracted via A_3. The signal was displayed in a CRO. Square pulses of current were delivered via the outermost electrodes. The total current was measured with A_4 in the current-to-voltage configuration which virtually grounded the bath. The voltage pulse applied and the total current flowing across the membrane were simultaneously recorded

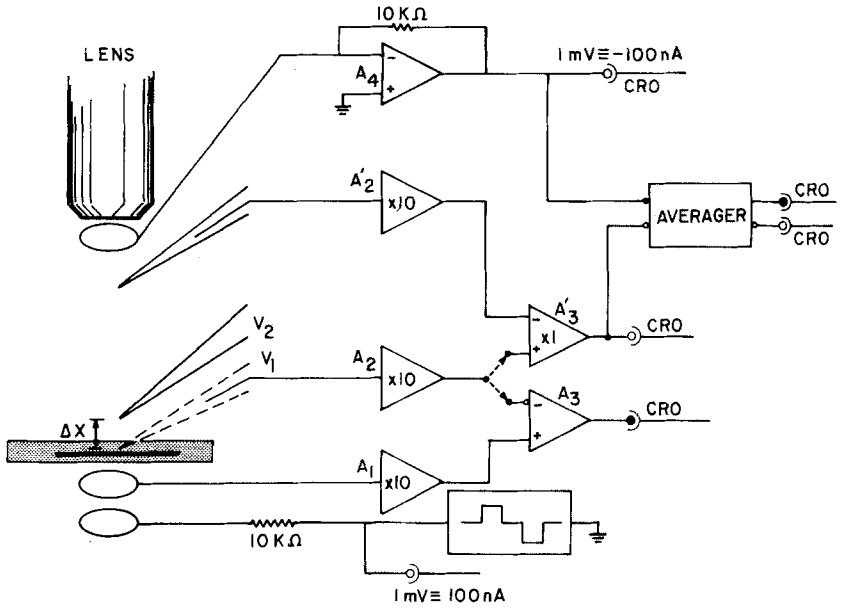

Fig. 2. Electrical diagram for electric field scanning. The disk containing the monolayer was mounted horizontally as a flat sheet in a shallow Lucite chamber. The chamber was placed on the stage of a microscope. (i) *Current injection:* biphasic current pulses were passed across the membrane. The total current was measured via A_4 in the current-to-voltage configuration which virtually grounded the bath. These pulses were recorded in a CRO and accumulated in a digital averager. (ii) *Total resistance:* voltage drop across the membrane was recorded via A_1 and A_2 amplifiers and differentially substracted in A_3. (iii) *Voltage scanning:* signals were recorded with two microelectrodes, a moving one placed near the MDCK monolayer (V_1) and a remote one. They were recorded via A_2 and A_2' substracted in A_3' and accumulated in a digital averager. A total of 512 pulses were collected. The microelectrode was then lifted 8 μm (V_2) and a second set of 512 pulses were collected and substracted from the previous set

Our observations reveal that the occluding junctions of MDCK cells are heterogeneous, i.e., sites of high conductance alternate with regions of low conductance. This functional heterogeneity correlates with the irregular structure of occluding junctions as seen in freeze-fracture replicas. The latter show regions where the junction consists of as many as 10 junctional strands in some regions, changing abruptly within the same junction to areas only formed by 1 or 2 ridges. Therefore, occluding junctions of MDCK cultured monolayers are functionally and morphologically heterogeneous, with "tight" regions intermixed with "leaky" ones.

Materials and Methods

Formation of the MDCK Monolayer

MDCK cells in the 100 to 110th passage were grown at 36.5 °C in roller bottles with an air-5% CO_2 atmosphere and 100 ml of Complete Eagle's Minimal Essential Medium (CMEM) with Earle's salts (Grand Island Biological Co. (GIBCO) F-11, Grand

Island, N.Y.), 100 U/ml of penicillin, 100 μg/ml of streptomycin and 20% calf serum (GIBCO) 617. As discussed in previous papers (Misfeldt et al., 1976; Cereijido et al., 1978*a* and *b*), the electrical resistance of these monolayers is around 100 Ωcm^2. Yet it was noticed that cells of a lower passage, 54–65 monolayers, have a much higher resistance (400–1500 Ωcm^2). Barker and Simons (1978) have recently communicated resistance of up to 4166 Ωcm^2 in MDCK monolayers of 61–66 passages. Cells were harvested with trypsin-EDTA (GIBCO 540) and plated on discs of a nylon cloth (HC-103 Nitex, Tetko, Inc. Elmsford, N.Y.) coated with collagen extracted from rat tails by the method of Bornstein (1973). Once sterilized under UV light, each disk was placed into a 16-mm well of a multichamber disk (Linbro Chemical, New Haven, Conn.), and a suspension of MDCK cells in 1.0 ml of CMEM was added to a density of 4×10^5 cells/cm^2. After incubation for 90 min at 36.5 °C in an air-5% CO_2 atmosphere with constant humidity (V.I.P. CO_2 Incubator 417, New Brunswick, New Jersey) to allow for attachment of the cells, disks were transferred to other multidish chambers containing fresh CMEM without cells. A continuous monolayer was thus formed. The fact that the disk supporting the monolayer is permeable and transparent permits a direct observation under an optical microscope and the injection of electric current to study membrane resistance. The electrical resistance across the monolayers starts to develop approximately 5 hr after plating and reaches a steady value in about 20–24 hr (Cereijido et al., 1978*a* and *b*). All monolayers used in the present study were plated for 2–6 days.

Morphological Studies

For light microscopy, cultures of MDCK cells were grown to confluency on # 1 coverslips placed in plastic Petri culture dishes. After 48 hr, the coverslips were lifted with fine tweezers and placed, with the monolayer facing down, on a glass slide where a drop of medium was previously added. A bridge of paraffin was placed in order to avoid direct contact between the cells and the surface of the slide. The preparation was then sealed with melted paraffin and bee wax, and was used for observation periods ranging from 30 min up to 1 hr. A Zeiss Photomicroscope II, equipped with phase-contrast optics and differential interference-contrast (Nomarski) optics, was used. For the latter, a 100 X Planachromatic objective was used. Photomicrographs of the living monolayer were recorded with Panatomic film (Kodak) using a green filter.

Freeze-fracture replicas were obtained from monolayers fixed with 2.5% glutaraldehyde for 30 min, and gradually infiltrated with glycerol up to 20% concentration, where they were left for 1 hr. The cultures were then detached from the substrate and the isolated monolayers frozen in the liquid phase of Freon 22 cooled with liquid nitrogen. Freeze-fracture was carried out using a 301 Balzers apparatus equipped with a turbomolecular pump, at −120 °C, and a vacuum of 2×10^{-6} mm Hg. After evaporation of platinum and carbon, replicas were recovered in sodium hypochlorite, washed in distilled water, and mounted on Formvar coated 100-mesh grids. Further details on the technique have been published (Martínez-Palomo, Chávez & González-Robles, 1978). Observations were carried out with a Zeiss EM10 electron microscope. All micrographs of replicas are shown with the shadow direction from bottom to top.

Electrophysiological Methods

Total membrane resistance and capacity (Fig. 1). The disk containing the monolayer was mounted as a diaphragm between two Lucite chambers of 2.5 ml each. The exposed area was 0.2 cm^2. Current was delivered from a square pulse generator whose output was connected to a chlorided silver electrode via a 10 kΩ resistor. It was collected through a second electrode placed on the opposite chamber, which was virtually grounded via a current-voltage converter with a 10 kΩ resistor in the negative feedback loop. The current pulse was displayed in a cathode ray oscilloscope (CRO). The voltage deflection across the preparation reproduced by the current flow was measured with two chlorided silver electrodes placed at less than 1 mm from each side of the monolayer. They were connected to high input impedance amplifiers (voltage-follower A_1 and A_2). The signals were substracted with a differential amplifier (A_3), and recorded on the same screen of the CRO used to display the current pulse. The position of the recording electrodes was fixed and the same in all experiments in order to substract the contribution produced by current flow through the saline and the Nylon disk with collagen but without the MDCK monolayer. Thus the I/V curve reported were corrected for this contribution.

Electric field scanning along the apical border (Fig. 2). The disk was horizontally mounted in between two flat Lucite chambers. The exposed area was 0.2 or 0.65 cm^2. The chamber was placed on the stage of a microscope and was flat enough to permit observation of the monolayer. The preparation was visualized with a Zeiss water immersion objective (40/0.75 W) with a long working distance, which permits both a clear view of the intercellular spaces and the positioning of the exploring microelectrode. This electrode was held by a piezoelectric ultramicromanipulator (E. Licht, Denver, Colo.) mounted on a conventional micromanipulator (Narishige, MK2). The ultramicromanipulator was adjusted to produce a lift of 8 μm of the tip of the microelectrode when a 6-V pulse was applied. In order to avoid oscillations of the tip, this pulse was rounded with a time constant of ca. 1 sec. Microelectrodes were filled with 3 M KCl and, after beveling, had a resistance of 5–10 MΩ. Once the tip of the microelectrode was located barely touching the desired spot on the apical border (noticeable by the spurious noise), a set of 512 pulses of current were passed and the voltage deflections at the tip of the exploring microelectrode were recorded and accumulated in a Nicolet digital averager (Instruments Corp. Madison, Wisc.). The microelectrode was then raised 8 μm and a second set of 512 pulses were passed, and again the potentials at the microelectrode were collected and substracted from the first series. These signals were differentially recorded (A_2, A_2' and A_3'), refered to a second microelectrode positioned 200–500 μm above. Signals were digitalized in the averager with 9 bit resolution, at 40 μsec per point and with a time constant of 0.1 to 1 msec. This procedure was adopted to improve the signal-to-noise ratio. As a control of the pulse protocol the pulses of injected current were also fed into the averager and substracted, thus leading to no detectable signal. Short pulses with a positive and a negative deflection were sent to avoid ion accumulations. Each deflection lasted 5–10 msec. Unless otherwise stated, their intensity was 20–50 μA cm^{-2}. The set-up used to deliver and measure current was equal to the one depicted in Fig. 1. Total membrane resistance was also measured in a similar way with amplifiers A_1 and A_2.

Amplifiers A_1, A_2, A_2' and A_4 were made with FET input operational amplifiers (1026 Teledyne Philbrick; Dedham, Mass.) and A_3 and A_3' with FET input instrumentation amplifiers (AD 521, Analog Devices, Norwood, Mass.).

Results

Morphological Observations

Light microscopy. Living cultures of MDCK cells grown on cover slides form a single layer of polyhe-

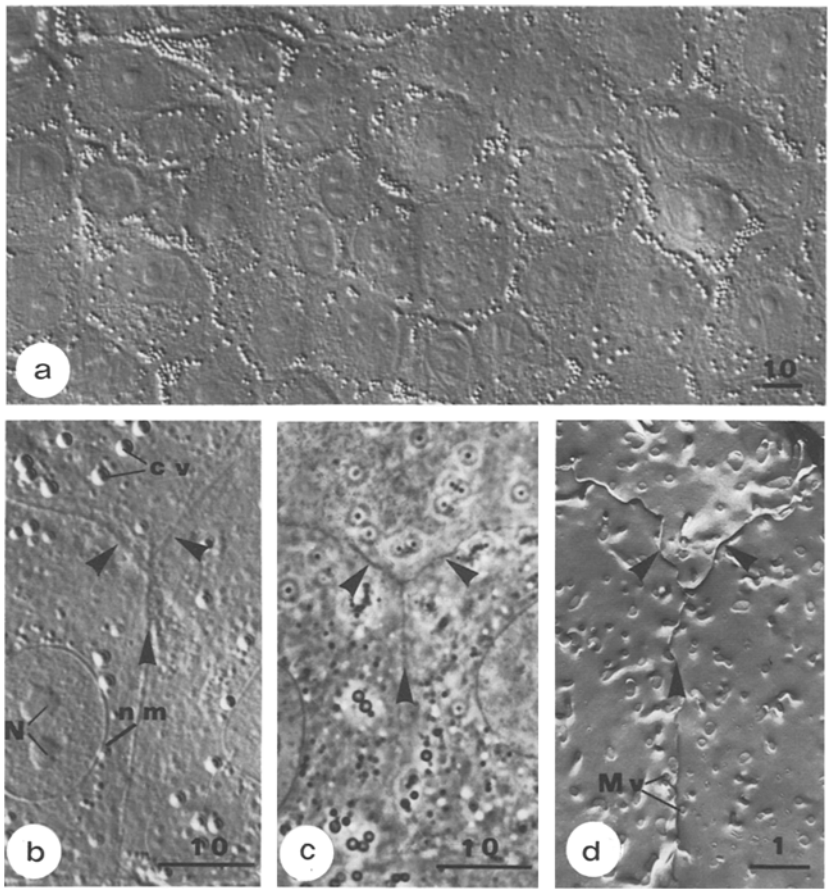

Fig. 3. Surface views of confluent MDCK monolayers. With Nomarski optics the outlines of the individual cells can be readily identified (*a* and *b*). Other cellular details revealed by this technique are the nuclear membrane region (*nm*) the nucleoli (*N*) and the cytoplasmic vacuoles (*cv*). The region of cell-to-cell apposition appears as an elevated ridge, identified with Nomarski optics at a plane located near the lumenal surface of the monolayer. In the field shown in *b*, the ridges limiting three cells are seen (arrowheads). The intercellular space can also be visualized in living monolayers with phase contrast optices (*c*) as an uninterrupted dense line (arrowheads). For purposes of comparison, a region of intersection between three MDCK cells at the lumenal region of the plasma membrane is shown in a freeze-fracture replica of *E* faces (*d*). Notice that the dense cellular outline seen with light microscopy of living cells corresponds to the region where the tortuous lateral membranes converge. The region of intercellular apposition is bound by abundant cross sectioned microvilli (*Mv*). Scales represent μm. *a*, 700×; *b*, 1,300×; *c*, 1,600×; *d*, 10.000×

dral cells, tightly adhered both to the substrate and to each other (Fig. 3*a*). The regions of cell-to-cell apposition appeared with Nomarski optics (Fig. 3*b*) as slightly elevated ridges, that in some regions had a beaded appearance. The extremely shallow depth of field of the Normarski optics clearly showed that the ridge is limited to the most lumenal side of the lateral intercellular space, immediately below the apical surface of the cultured cells, where the circular profiles of microvilli were identified. Similar regions could be visualized with phase-contrast microscopy of living monolayers (Fig. 3*c*). The intercellular space appeared with the latter method as an uninterrupted dark line of irregular thickness. However, the depth of field was not as restricted as with Nomarski optics, and, therefore, the plane of the dense intercellular outline could not be limited with phase contrast by fine focusing to the upper region of the lateral intercellular space.

Both the intercellular ridge seen with Nomarski optics and the dense line observed with phase contrast microscopy corresponded to the region where the occluding junction is located between adjacent MDCK cells. However, it is not the junction itself that is visualized with these light microscopical techniques. For purposes of comparison, Fig. 3*d* shows an intercellular region as seen in freeze-fracture replicas of the *E* face of MDCK plasma membranes. It becomes evident that the outline observed with light microscopy corresponds to the region of cell-to-cell attachment at the lumenal side of the monolayer. At this region of cell contact, the converging membranes follow a tortuous path laterally limited by numerous microvilli. It is the superposition of the adjacent sinuous membranes and the converging microvilli that give rise to an optically visible outline detected with the light microscope. Our observations indicate that the region where the occluding junction is located can be visualized with light microscopy, but that even under the best conditions of resolution the occluding junction itself cannot be observed with light microscopical methods.

Membrane Capacity

Figure 4 shows the time course of the voltage variation produced by a step passage of current both in

the collagen disk without (upper) and with (lower) the monolayer. The dashed line divides the deflection caused by the support from that of the monolayer itself. From this kind of recording a capacity of 1.4 μF cm^{-2} was calculated. This value indicates that the cells over all the available area and leave no empty spaces (a point verified by light microscopy) and that the membrane has a capacity within the same range of natural epithelia (Finkelstein, 1964; Fishman & Macey, 1968; Cuthbert & Painter, 1969, Schanne & Ruíz-Ceretti, 1978).

Current-Voltage Relation (I/V curves)

The electrical resistance across epithelial membranes may be a function of both the intensity and the duration of the pulses injected. Therefore, we explored whether these parameters in the voltage scanning may introduce changes in the junctional complexes as revealed by their electrical resistance. Current voltage curves obtained with MDCK monolayer bathed in CMEM were linear and symmetrical (Fig. 5) within the range explored (± 2 mA cm^{-2}) and did not reach saturation, suggesting that ion transfer is not operated by charged carriers, but proceeds mainly through ionic channels (Conti & Eisenman, 1965, 1966; Eisenman, Sandblom & Walker, 1967). This agrees with previous observations by Cereijido et al. (1978*a* and *b*).

Leaky epithelia can exhibit marked time-dependent polarization effects (Wedner & Diamond, 1969; Wright, Barry & Diamond, 1971). In order to explore whether the duration of the current pulses could influence the electrical resistance of the MDCK monolayer, the *I/V* curves were also studied with short (5 msec) and long current pulses (2.2 sec) in the same monolayers. As illustrated in Fig. 6, in both cases the curves were symmetrical and linear. This indicates that the conducting spots described below were normally present and were not induced by the passages of strong currents. In the experiments reported below, we passed currents of low density (20–50 μA cm^{-2}) and short duration (10 msec).

Detection of Local Electric Fields and Conductive Spots

As described above, the scanning method is based on the detection of a voltage difference between two points: one barely touching the conductive spot of the monolayer and the other 8 μm above. It is expected that, if current does not flow homogeneously through all points of the surface, but only through discrete regions (e.g., an occluding junction), current density will increase at these levels and then disperse as the distance from the monolayer increases. Figure 7 shows that when the cell monolayer is absent, current pulses as intense as 530 μA cm^{-2} fail to elicit a detectable signal (above) and current densities of 1600 ΩA cm^{-2} are necessary to produce a clear voltage deflection (below). By comparison, most of the pulses used to scan MDCK monolayers were of 20–50 μA cm^{-2}. In this experiment $J_s = E/\rho_s$, where J_s is the current density in the saline (A cm^{-2}), E the electric field (V cm^{-1}) and ρ_s is the resistivity of the saline (Ωcm). J_s can be directly measured and E can be calculated from the voltage deflections across the saline ΔV_s when the exploring microelectrode is raised 8 μm(ΔX) using the equation $E = \Delta V_s/\Delta X$. Thus the experimental set-up can be verified by measuring ρ_s, which is a known value. We obtained a value of 60 Ωcm, which is close to the one expected for the bathing medium we used (62 Ωcm) indicating the adequacy of the experimental conditions.

Another point to be determined was the spatial resolution of the method. Figure 8 shows on the upper left the silhouette of a cell and its neighbors and the line along which the voltage was scanned. The junction on the right-hand side of the cell (second point from right to left) was a very conductive one. The record obtained at that point is shown in Fig. 8-*1*. The upper trace resulted by substracting the second (8 μm above) from the first (barely touching the monolayer), and indicates that the density of the current at the two points was different. The lower trace on the same photograph resulted from the substraction of the two sets of current pulses, and the fact that this procedure left no detectable signal indicates that they were identical and that the upper trace may not be adscribed to differences in the current injected. This verification was done routinely and is represented in each picture by the horizontality of the lower trace. The scanning in this particular experiment was performed with a current of 20 μA cm^{-2}, and the fact that this current through the MDCK monolayer elicited a clear signal, while a current of 530 μA cm^{-2} failed to do so when the membrane was absent (Fig. 7) indicates that current was channeled to discrete points where it was condensed. The amplitude of the signals is represented in the graph at the bottom left of Fig. 8. In order to compare the amplitude of the signals obtained in different monolayers with different applied currents, we express the signals as current density (J_j, in A cm^{-2} is equal to E/σ_s, where E is the electric field, and ρ_s is the resistivity of the saline) divided by the potential difference across the monolayer (ΔV_e). Therefore, the amplitude of the signal is given in $A\ V^{-1}\ cm^{-2}$, the units being mho cm^{-2}. It may be noticed that

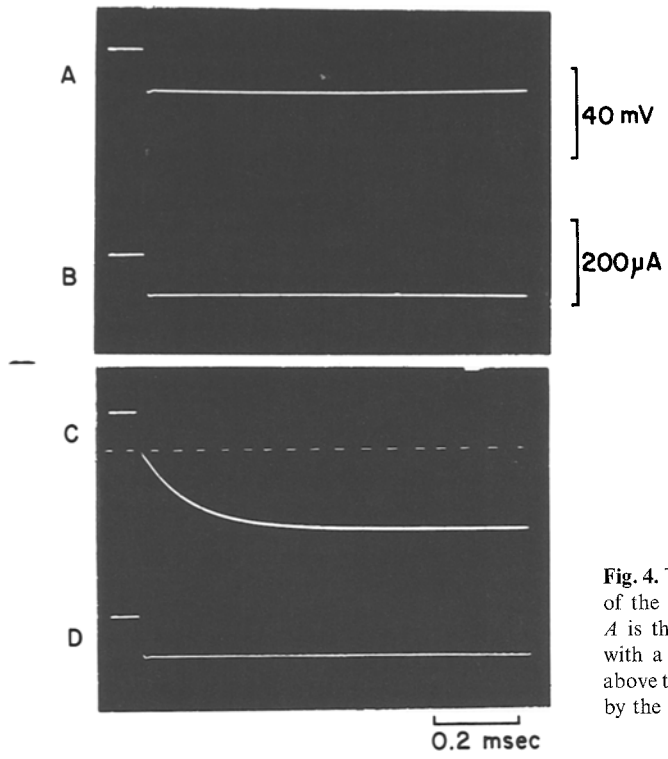

Fig. 4. Total membrane capacity and resistance: *B* and *D* are the recordings of the injected current as recorded with the circuit depicted in Fig. 1. *A* is the *IR* drop across the saline and the empty disk; *C* is the drop with a disk containing an MDCK monolayer. Note in *C* the *IR* drop above the dashed line, the voltage drop across the membrane is represented by the portion of the curve below the dashed line

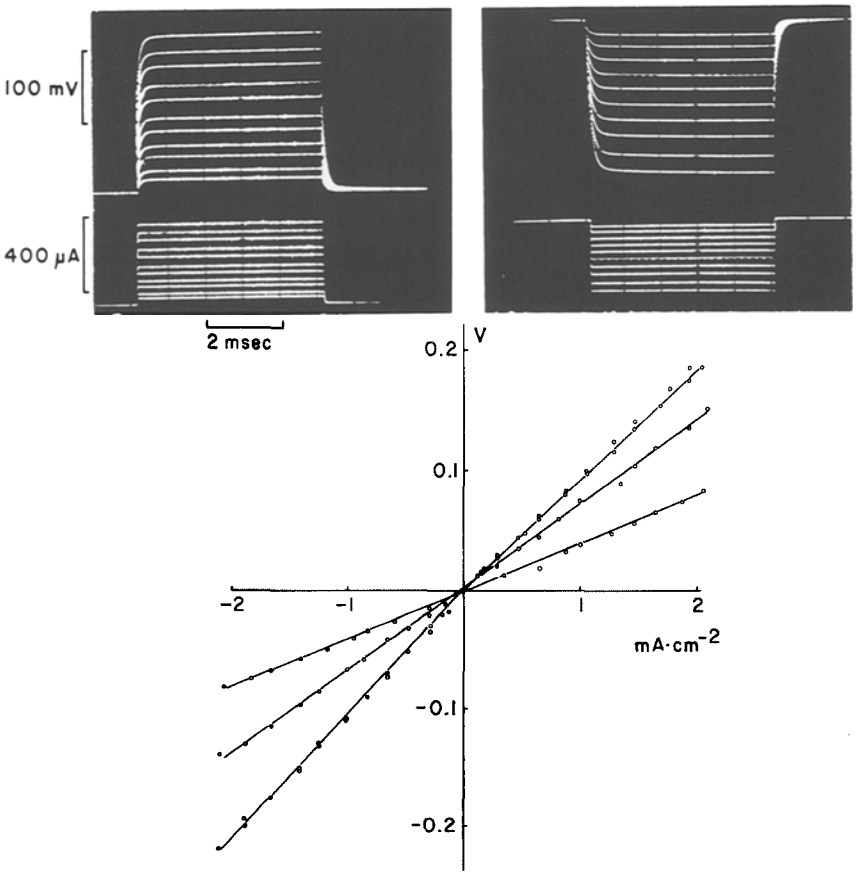

Fig. 5. Current-voltage relation of the whole MDCK monolayer as recorded with the circuit depicted in Fig. 1. The photographs show paired records of voltage (above) and current pulses (below). Positive deflections refer to the positivity of the apical border. The *I/V* curves shown at the bottom of the Figure correspond to four different monolayers fitted by three straight lines. The contribution of the empty disk and the bathing solution was substracted. Note that the *I/V* relation is linear in the range explored (± 2 mA cm^{-2})

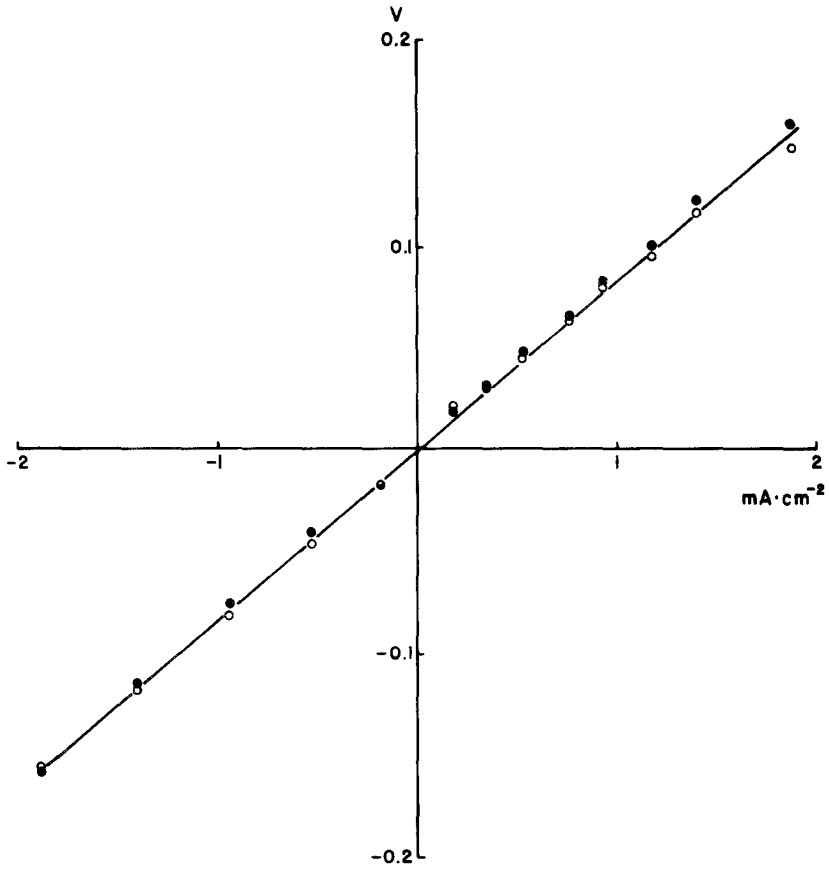

Fig. 6. Current-voltage relation of the whole MDCK monolayer for short (5 msec; filled circles) and long pulses (2.2 sec; open circles). Note the linearity and time independence of the I/V relation

at a few micrometers from the conductive junction the signal is attenuated by as much as 60% (record 2) and it completely vanishes at the center of the cells on the two sides. Interestingly, the junction on the opposite side of the same cell was not conductive (record 3).

Scanning of MDCK Monolayers

Figure 9 shows a region of a monolayer where the scanning was concentrated on the junctions and the center of the cells. Each picture corresponds to a spot marked with the same number on the silhouette. Starting with a nonconductive cell body (*1*) we found a highly conductive junctional region (*2*), then a nonconductive cell body (*3*), etc. The comparison of records *2* and *8* which were obtained on the same junction, but a couple of micrometers apart, indicates that an occluding junction may drastically vary its conductance along its length. Cells bodies were never conductive, and the small signal detected on some of them was invariably related to the incomplete dissipation of a neighboring spot with high conductance.

Figure 10 summarizes the results exclusively obtained on occluding junctions. Half of them, represented by the grey bar, escaped detection by our method ($<10^{-2}$ mho·cm^{-2}), suggesting that in 50% of its length the junction was functionally tight. The remaining 50% had a very low conductance with isolated spots of high permeability.

We have attempted to measure the resistivity of the junction in order to estimate whether ions move between the leaky regions of the junctions as in free solution. If this were the case, one would expect to measure a junction resistivity (ρ_j, Ωcm) close to one of the saline (ρ_s, 60 Ωcm). This evaluation was based on the current density measured at the junctions (J_j) and the potential difference across the whole monolayer (ΔV_e). As shown before, J_j was measured as E/ρ_s and the conductance per unit surface of junction was calculated from $J_j/\Delta V_e$. The potential difference across the epithelial cells (ΔV_e, would be the driving force generating the current J_j measured as a voltage drop across 8 μm of saline. The conductance per unit surface of junction was 0.69 ± 0.16 mho cm^{-2} (mean ± SE, $n=58$). To calculate the junction resistivity, we applied the known relation $R=\rho_j^l/_A$, where R is the resistance in ohm, ρ_j the resistivity of the junction (Ωcm), l the length of the junction (cm) and

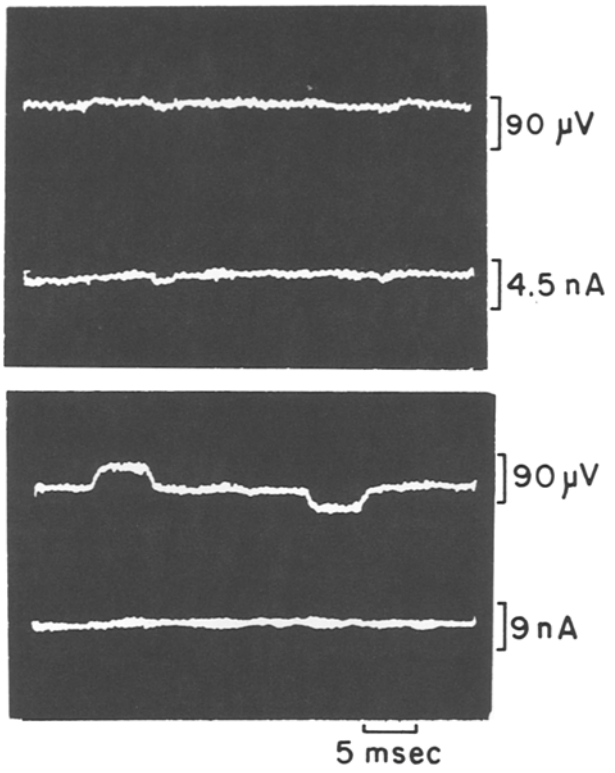

Fig. 7. Voltage drop across the saline. A nylon cloth disk coated with collagen containing no monolayer was mounted as in Fig. 2. In each photograph the upper tracer corresponds to voltage and the lower one to the current passed. As expected from the fact that each current curve results from the sustraction of two identical sets of pulses, no signal is detected. The substraction of the two sets of voltage deflections, one made 8 μm above the other, does not show a clear signal when the current is 0.53 mA cm^{-2} (upper set), but can be detected when the intensity is 1.6 mA cm^{-2} (lower set)

A its cross-section area (cm^2). From the studies of electron microscopy we took a value of l of 0.5 μm. The resulting resistivity of the junction was 2.9×10^4 Ωcm. This value is much higher than the one expected in the saline indicating than ion diffusion through the junction is restricted. Notice that this is a minimum estimate, because the 0.5 μm. corresponds to the average width of the belt occupied by the junction. Yet the strands themselves occupy a narrower band and the resistivity of the junction would be even higher than that of free solution. But even then the value will be much lower than 10^9 Ωcm, the resistivity of a typical cell membrane 8 nm thick and with a conductance of 1 mmho cm^{-2}.

Electron Microscopy

In freeze fracture replicas, confluent monolayers of MDCK cells usually showed large surfaces of lumenal or basal regions of the plasma membrane. Less frequently, the fracture path followed the lateral region of the plasma membrane and gave rise to replicas where considerable portions of lumenal and lateral regions were simultaneously exposed, thus giving a clear view of the distribution of the occluding junction. The junctions were not frequently exposed by the fracture of the frozen monolayer because they are located at the most lumenal side of the lateral membranes regions, where the plasma membrane follows in general an abrupt angle at the transition between the lateral and the lumenal sides. Furthermore, in contrast to most natural epithelia, the lateral aspect of MDCK plasma membranes represents only a small fraction of the lumenal and basal surface extension, a factor that also determines the relative scarcity of extensive regions of fractured lateral membranes.

In contrast to the regularity of the freeze-fracture pattern of occluding junctions in natural epithelia, in MDCK cells some junctions appeared constituted by only one or two junctional strands (Fig. 11*a*), while in others, junctional strands formed a much more complex membrane network constituted, in the apicobasal direction, by up to 10 strands. When the fracture plane was extensive enough, the structural heterogeneity of the occluding junction of MDCK cells became apparent: in a given cell, the number of strands of the occluding junctions were limited to 1 or 2, while in other regions of the perimeter of the same cell, the junction was formed by 6–8 ridges (Fig. 11*b*). In other cells up to 10 strands were found at a given region of the occluding junction, counted in the apico-basal direction. The junctional strands appear on *P* faces as segments of smooth ridges of various lenghts interconnected with linear arrays of membrane particles. On the complementary *E* faces the occluding junctional components appeared as linear furrows with abundant adherent particles. Therefore, the occluding junctions of MDCK resemble those seen in developing epithelia (Montesano et al., 1975; Suzuki & Nagano, 1978; Luciano, Thiele & Reale, 1979).

Discussion

The present observations indicate that the occluding junctions of the epithelial cell line MDCK are essentially tight and are studded with spots of high conductivity. The heterogeneity of the sealing properties of MDCK occluding junctions was detected with the use of an electric field scanning procedure of high spatial resolution, using pulses of current which do not modify the conductance of the junctions.

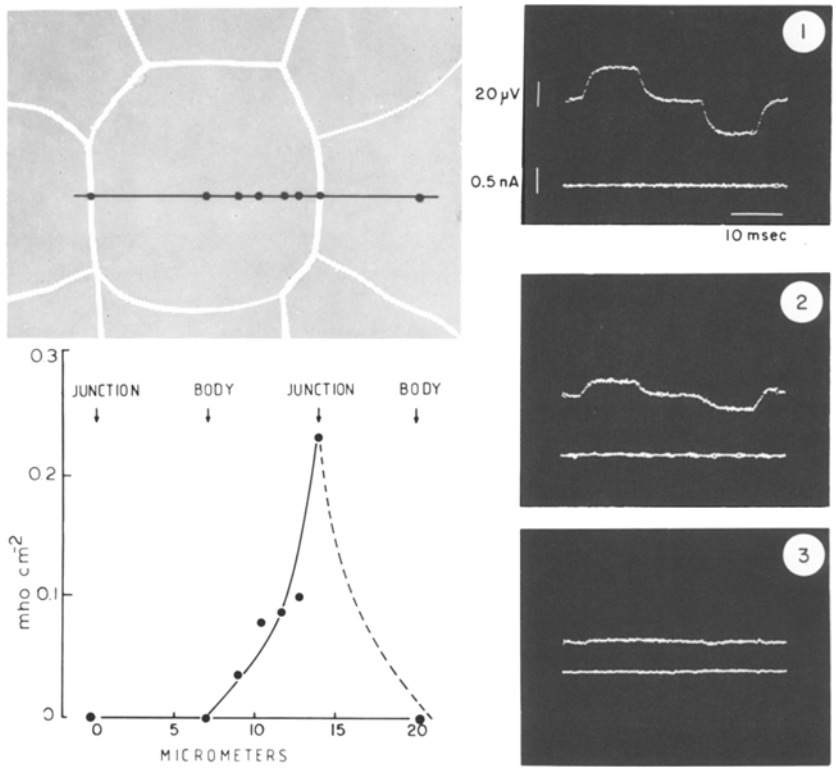

Fig. 8. Electric field scanning across a single cell showing the spatial resolution of the method. The total current density injected was 20 μA cm^{-2}. The left-hand side shows the silhouette of a cell with the points where the recordings were made. The amplitude of the signals obtained are represented below in a corresponding point. The records on the right-hand side illustrate the signal obtained when the microelectrode was placed on a conducting point on a tight (*1*), on the center of the cell (*3*), and on an intermediate point (*3*). As a routine control for the pulse protocol, the lower trace in each record shows the cancellation of pulses

Examination of freeze-fracture replicas of MDCK confluent monolayers revealed that the occluding junction is heterogeneous. Within the perimeter of a given cell, certain regions are made up of 6–10 junctional strands, while in others the number of strands is reduced to 1 or 2. Each region of variable junctional depth measured several micrometers in length. Quantitative data on the morphology of occluding junctions in freeze-fracture replicas will be the subject of a separate report (A. Martínez-Palomo, I. Meza, G. Beaty, and M. Cereijido).

Natural epithelia act as permeability barriers because adjacent cells come into close contact in a region designated by cytologists at the turn of last century as "terminal bar" (*see* Erlij and Martínez-Palomo, 1978, for a review). Electron microscopic examination of these regions revealed the apparent abscence of intercellular space between the membranes of neighboring cells at the "terminal bars", renamed occluding junctions (*zonulae occludentes,* or tight junctions), and that macromolecular tracers were stopped at the apical end of the junction (Farquhar & Palade, 1963).

The presence of one group of epithelia with high transmural resistance (tight epithelia) and a second group with low resistance (leaky epithelia) was pointed out by Clarkson (1967). The concept that leakiness in certain epithelia is an intrinsic attribute of tissues like the intestinal and the glallbladder mucosae arose from several lines of evidence. (i) Epithelia like the gallbladder exhibit a high rate of ion and water transport and have at the same time a very low ($\sim 30\,\Omega cm^2$) electrical resistance (Diamond, 1962; Diamond & Bossert 1967; Whitlock and Wheeler, 1964), indicating that low resistance does not necessarily imply damage of the preparation. (ii) It was observed that the sum of the apical plus the basolateral cell membrane resistance would confere to the epithelium an electrical resistance more than two orders of magnitude higher than the actual measured resistance, implying the existence of a shunt (Boulpaep, 1972; Frizzell & Schultz, 1972). (iii) The use in electron microscopy of lanthanum as an electron dense tracer of lower molecular weight than those used in earlier studies (Martínez-Palomo, Erlij & Bracho, 1971), indicated that under physiological conditions the tracer permeates the occluding junctions of some epithelia in which resistance is a few hundred ohms or less (Machen, Erlij & Wooding, 1972; Martínez-Palomo & Erlij, 1973; Tisher & Yarger, 1973). (iv) Finally, Frömter (1972) and Frömter and Diamond (1972), using a voltage scanning procedure, de-

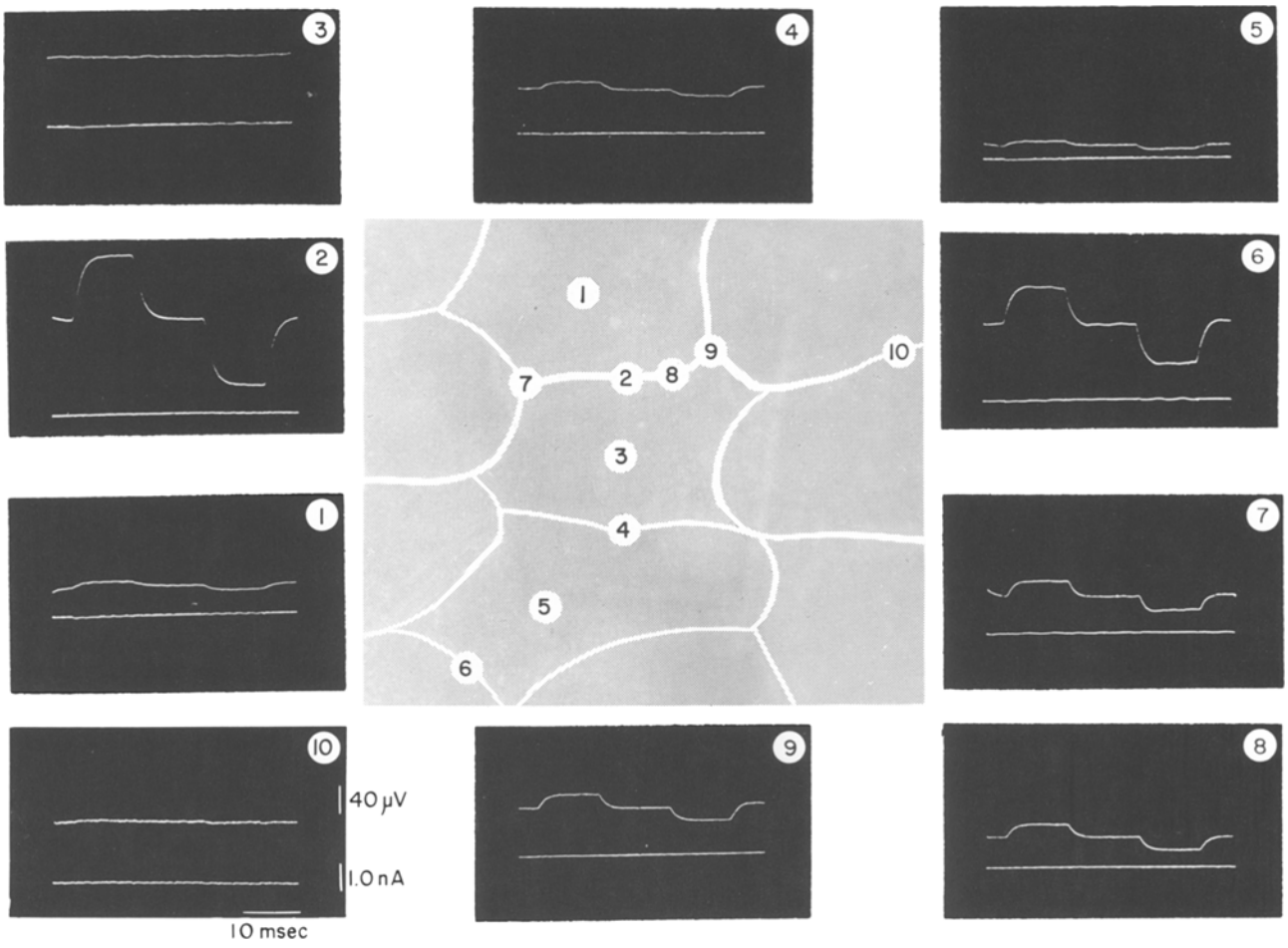

Fig. 9. Electric field scanning across the cells of a region of an MDCK monolayer showing the variability of conductive pathways. The method and the protocol used are described in Figs. 2 and 7, respectively. The position of each recording is indicated by the numbers. Note that the signals collected on the center of the cells are barely detectable (*1, 3* and *5*) and that a given junction can exhibit marked variations of its conductance within a few micrometers (*compare* recordings *2* and *8*). In this particular experiment the sets of pulses were of 1024 instead of 512 units

monstrated that occluding junctions are the site of shunt pathways in leaky epithelia.

The paracellular pathway is not simply a gap of free solution, but possesses a considerable degree of selectivity (Barry, Diamond & Wright, 1971; Asterita & Boulpaep, 1972; Moreno & Diamond, 1975; Reuss & Finn, 1975). Furthermore, the properties of a given junction do not remain constant, but adapt to physiological requirements and experimental conditions (Urakabe, Handler & Orloff, 1970; Erlij & Martínez-Palomo, 1972; DiBona & Civan, 1973; Pitelka et al., 1973; Wade, Revel & DiScala, 1973; Elias & Friend, 1976; Humbert et al., 1976; Spring & Hope, 1978). They may also be subject to hormonal control (Picket et al., 1975, Tice, Wollman & Carter, 1975). Occluding junctions not only control the flux of substances through the paracellular pathway, but, through the shunting of electrical potentials, they influence the active transport across the membranes of the epithelial cells as well (Reuss & Finn, 1976; Civan & DiBona, 1978; Finn & Bright, 1978).

In view of the functional heterogeneity of the occluding junction, attempts were made to correlate the details of its structure with its permeability properties. Friend and Gilula (1972) found clear-cut morphological differences between the number of junctional membrane strands among various epithelia. Later on, Claude and Goodenough (1973) reviewed a series of epithelia and found an apparent quantitative correlation between junctional morphology observed in freeze-fracture replicas and the electrical resistance. Claude (1978) put forward a theoretical model and considered that the relationship between the number of junctional strands and the transmural resistance

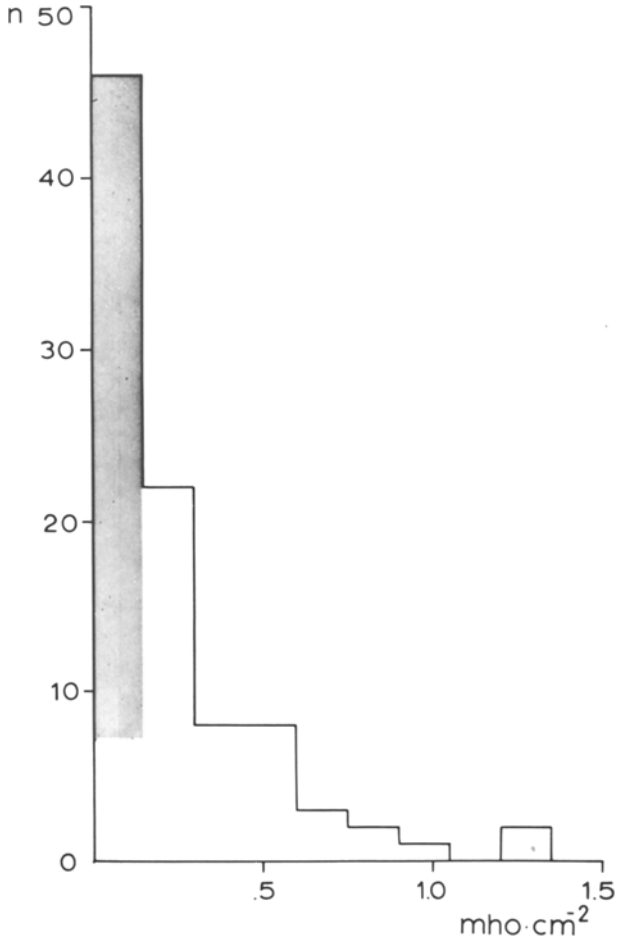

Fig. 10. Histogram of the signal amplitude of 92 intercellular junctions. Values were normalized to the total current density used. The shaded column corresponds to recordings below detection (10^{-2} mho cm^{-2})

appears to be exponential. However, Martínez-Palomo and Erlij (1975) have shown that epithelia with junctions having a similar number of strands may have resistances differing by more than two orders of magnitude and that occluding junctions in a tight epithelium can be reversibly opened without altering the freeze-fracture pattern of the junction. Furthermore, the developing choroid plexus shows changes in permeability properties without modification of the freeze-fracture pattern of the occluding junctions (Mollgard, Malinowska & Saunders, 1976). In fact, the conductive element may be a channel across the strand and, therefore, the number of open channels in a strand may determine its conductance (Claude, 1978). However, it is clear that when the comparison is exclusively restricted to epithelia of extreme low and high resistance, i.e., the proximal tubule of the kidney (one of the leakier epithelia) and the frog skin (one of the tighter epithelia), the difference in the number of junctional strands is evident (Claude & Goodenough, 1973; Pricam, et al., 1974; Kuhn & Reale, 1975).

The leakiness of the MDCK monolayer, as a whole, and the high conductive sites detected with the electric field scanning procedure may not be due to imperfect sealing of intercellular space, since the monolayer has a 2 to 1 discrimination between K^+ and Li^+ and the process is reversibly sensitive to changes in pH (Cereijido et al., 1978*a* and *b*). This is in keeping with the fact that even the leakiest junctions of this preparation have a resistivity one order of magnitude higher than the free solution. Several authors have observed that junctions that are normally low conducting, like those of the frog skin, can be opened by the passage of a strong electric current (Mandel & Curran, 1972; Bindslev, Tormey & Wright, 1974). Yet, this factor may not have produced the conductive spots observed in this study as the current/voltage curves remain linear up to pulses 100-times greater and 60 times longer than the one used to localize conductive areas. It may be pertinent to recall that, even in the points of highest conductance, the diffusion of ions is restricted to less than one tenth of the values in free solution, indicating that they are not crossing a free water channel.

The junctions of MDCK monolayers are morphologically heterogeneous, as revealed by freeze-fracture. Regions of high conductance may well correspond to the sites of the occluding junctions constituted by 1–2 junctional strands in freeze-fracture. The sites of low conductance may be the junctional regions constituted by up to 10 strands. Regional variations in the number of strands of a given occluding junction have been observed in epithelia like the rabbit gallbladder (Claude & Goodenough, 1973), cultured mouse mammary gland (Pickett et al., 1975), and the fetal rat thyroid (Tice, Carter & Cahill, 1977). However, in these examples no evidence was obtained to correlate the heterogeneity in the number of strands of the occluding junctions with local variations in transepithelial conductance, as shown here for MDCK cultured monolayers.

When the MDCK monolayers develop on a nonpermeable support, they form focal blisters due to ion and water accumulation between the monolayer and the support. This reflects cyclical activity of the cells or differences in the attachment to the substratum, but not heterogeneity in their population (Rabbito et al., 1978). The existence of blistering and nonblistering patches does not correspond to the presence of conductive and nonconductive spots described in the present paper. While blisters cover an area of several dozens of cells, the variations in conductance

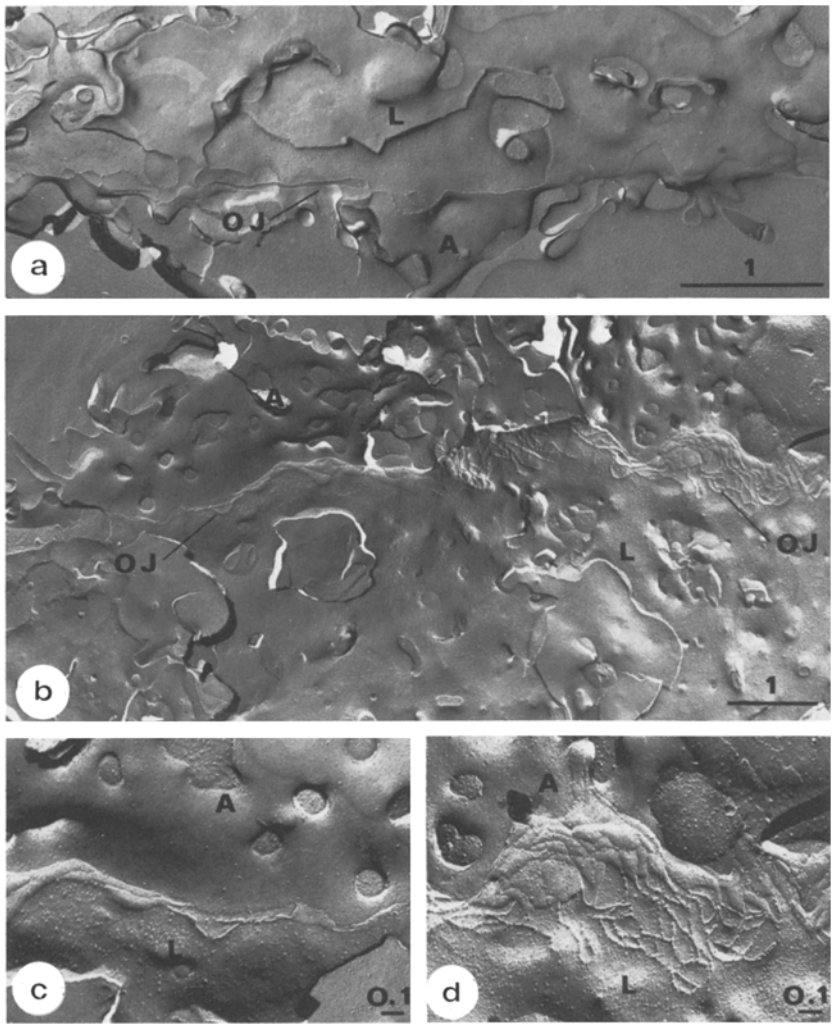

Fig. 11. Freeze-fracture replicas of MDCK monolayers grown at confluency. The occluding junctions may be formed by 1–2 strands (*a*). In some regions (left-hand side, *b*) the junction is formed by two strands, while in another region of the same cell (right-hand side) the occluding junction is constituted by a network of 6–8 strands. *c* shows a higher magnification of the occluding junctions in *b*, where only 2–3 strands constitute the junctions; the region where the junctional strands are more numerous (6–8) is shown in *d*. *A*, apical side of the plasma membranes; *L*, lateral side of the plasma membrane; *OJ*, occluding junction. Scales represent μm. *a*, 24,000×; *b*, 15,000×; *c*, 40,000×; *d* 40,000×

and number of strands, here reported, were detected along the perimeter of a single cell and within a few micrometers. On the contrary, the distribution of conductive and nonconductive spots over the whole area supports the idea of an homogeneous monolayer.

Obviously, MDCK cells are able to synthesize junctional elements, and the heterogeneity in the distribution of the strands does not seem to be due to genetic defects in the synthetic process. Local variations in the number of strands along the length of the occluding junction may reflect irregularities in the assembly process of the already synthesized membrane components. In this respect, studies by Meza et al., *(unpublished results)* indicates that cytoskeletal components, which may determine the topographical distribution of certain membrane elements, appears to be related to the sealing capacity of the occluding junctions in MDCK monolayers. Therefore, the structural and functional heterogeneity of MDCK occluding junctions may be the result of an incomplete assembly of membrane junctional components.

We wish to thank Lic. Leonardo Nicola Siri for his valuable advice and discussion of our work, Amparo Lázaro and Roberto Carmona for their efficient technical assistance and the CONACyT of México for research grants number 1508 and 059 from the PNCB and AM 26481 from N.I.H.

References

Asterita, M.F., Boulpaep, E.L. 1972. Ion selectivity of the paracellular pathway in *Necturus* proximal tubule. *Biophys. J.* **15**:229*a*

Augustus, J., Bijaman, J., van Os, C.H., Slegers, J.F.G. 1977. High conductance in an epithelial membrane not due to extracellular shunting. *Nature (London)* **268**:657

Barker, G., Simmons, N.L. 1978. Cell monolayers can display properties similar to high resistance epithelia. *J. Physiol. (London)* **285**:48*P*

Barry, P.H., Diamond, J.M., Wright, E.M. 1971. The mechanism of cation permeation in rabbit gallbladder. *J. Membrane Biol.* **4**:358

Bindslev, N., Tormey, J. McD., Wright, E.M. 1974. The effects of electrical and osmotic gradients on lateral intercellular spaces

and membrane conductance in a low resistance epithelium. *J. Membrane Biol.* **19**:357

Bornstein, M.B. 1973. Organotypic mammalian central and peripheral nerve tissue. *In:* Tissue Culture. P.F. Kruse and M.K. Patterson, Acad. Press. N.Y., Chapter 12, p. 86.

Boulpaep, E.L. 1972. Electrophysiological techniques in kidney micropuncture. *Yale J. Biol. Med.* **45**:397

Cereijido, M., Ehrenfeld, J., Meza, I., Martínez Palomo, A. 1979. Structural and functional membrane polarity in cultured monolayers of MDCK cells. *J. Membrane Biol. (in press)*

Cereijido, M., Robbins, E.S., Dolan, W.J., Rotunno, C.A., Sabatini, D.D. 1978*a*. Polarized monolayers formed by epithelial cells on a permeable and transluscent support. *J. Cell. Biol.* **77**:853

Cereijido, M., Rotunno, C.A., Robbins, E.S., Sabatini, D.D. 1978*b*. Polarized epithelial membranes produced *in vitro*. *In:* Membrane Transport Processes. Vol.I. J.F. Hoffman, editor. Raven Press, New York

Civan, M.M., DiBona, D.R. 1978. Pathways for movement of ions and water across toad urinary bladder. III. Physiologic significance of the paracellular pathway. *J. Membrane Biol.* **38**:359

Clarkson, T.W. 1967. The transport of salt and water across isolated rat ileum. Evidence for at least two distinct pathways. *J. Gen. Physiol.* **50**:695

Claude, P. 1978. Morphological factors influencing transepithelial permeability: A model for the resistance of the *zonula occludens*. *J. Membrane Biol.* **39**:219

Claude, P., Goodenough, D.A. 1973. Fracture faces of *zonulae occludentes* from "tight" and "leaky" epithelia. *J. Cell. Biol.* **58**:390

Conti, F., Eisenman, G. 1965. The steady-state properties of an ion exchange membrane with fixed sites. *Biophys. J.* **5**:511

Conti, F., Eisenman, G. 1966. The steady-state properties of an ion exchange membrane with mobile sites. *Biophys. J.* **6**:227

Cuthbert, A.W., Painter, E. 1969. Independent action of antidiuretic hormone on cell membranes. Voltage transient studies. *Br. J. Pharmacol. Chemother.* **35**:29

Diamond, J.M. 1962. The mechanism of solute transport by the gallbladder. *J. Physiol. (London)* **161**:474

Diamond, J.M., Bossert, W.H. 1967. Standing-gradient osmotic flow. *J. Gen. Physiol.* **50**:2061

DiBona, D.R., Civan, M.M. 1973. Pathways for movement of ions and water across toad urinary bladder. I. Anatomic site of transepithelial shunt pathways. *J. Membrane Biol.* **12**:101

Eisenman, F., Sandblom, J.P., Walker, J.L. 1967. Membrane structure and ion permeation. *Science* **155**:965

Elias, P.M., Friend, D.S. 1976. Vitamin-A-induced mucous metaplasia. An *in vitro* system for modulating tight and gap junction differentiation. *J. Cell. Biol.* **68**:173

Erlij, D., Martínez-Palomo, A. 1972. Opening of tight junctions in frog skin by hypertonic urea solutions. *J. Membrane Biol.* **9**:229

Erlij, D., Martínez-Palomo, A. 1978. Role of tight junctions in epithelial function. *In:* Membrane Transport in Biology. G. Giebisch, D.C. Tosteson, and H.H. Ussing, editors. Vol. 3, p. 27, Springer Verlag, Berlin

Farquhar, M.G., Palade, G.E. 1963. Junctional complexes in various epithelia. *J. Cell. Biol.* **17**:375

Finkelstein, A. 1964. Electrical excitability of isolated frog skin and toad bladder. *J. Gen. Physiol.* **47**:545

Finn, A.L., Bright, J. 1978. The paracellular pathway in toad urinary bladder: Permselectivity and kinetics of opening. *J. Membrane Biol.* **44**:67

Fishman, H.M., Macey, R.I. 1968. Calcium effects in the electrical excitability of "split" frog skin. *Biochim. Biophys. Acta* **150**:482

Friend, D.S., Gilula, N.B. 1972. Variations in tight and gap junctions in mammalian tissues. *J. Cell Biol.* **53**:758

Frizzell, R.A., Schultz, S.G. 1972. Ionic conductances of extracellular shunt pathway in rabbit ileum influence of shunt on transmural sodium transport and electrical potential differences. *J. Gen. Physiol.* **59**:318

Frömter, E. 1972. The route of passive ion movement through the epithelium of *Necturus* gallbladder. *J. Membrane Biol.* **8**:259

Frömter, E., Diamond, E.J. 1972. Route of passive ion permeation in epithelia. *Nature New Biol.* **235**:9

Handler, J.S., Perkins, F.M., Johnson, J.P. 1979. Studies of renal cell function using cell culture techniques. *Am. J. Physiol. (in press)*

Humbert, F., Grandchamp, A., Pricamm, C.,, Perrelet, A., Orci, L. 1976. Morphological changes in tight junctions of *Necturus maculosus* proximal tubules undergoing saline diuresis. *J. Cell Biol.* **69**:90

Kuhn, K., Reale, E. 1975. Junctional complexes of the tubular cells in the human kidney as revealed with freeze-fracture. *Cell Tissue Res.* **160**:193

Luciano, L., Thiele, G., Reale, E. 1979. Development of follicles and of occluding junctions between the follicular cells of the thyroid gland. *J. Ultrastruc. Res.* **66**:164

Machen, T.E., Erlij, D., Wooding, F.B.P. 1972. Permeable junctional complexes. The movement of lanthanum across rabbit gall-bladder and intestine. *J. Cell. Biol.* **54**:302

Madin, S.H., Darby, N.B. 1958. *As catalogued in:* American Type Culture Collection Catalog of Strains. **2**:47

Mandel, L.J., Curran, P.F. 1972. Response of the frog skin to steady state voltage clamping. I. The shunt pathway. *J. Gen. Physiol.* **59**:503

Martínez-Palomo, A., Chávez, B., González-Robles, A. 1978. The freeze fracture technique: Application to the study of animal plasma membranes. *In:* Electron Microscopy. Vol. 3, p. 503. State of the Art Symposia. J.M. Sturgess, editor. Microscopical Society of Canada. Imperial, Ontario

Martínez-Palomo, A., Erlij, D. 1973. The distribution of lanthanum in tight junctions of the kidney tubule. *Pfluegers Arch.* **343**:267

Martínez-Palomo. A., Erlij, D. 1975. Structure of tight junctions in epithelia with different permeability. *Proc. Nat. Acad. Sci. USA* **72**:4487

Martínez-Palomo, A., Erlij, D., Bracho, H. 1971. Localization of permeability barriers in the frog skin epithelium. *J. Cell. Biol.* **50**:277

Misfeldt, D.S., Hammamoto, S.T., Pitelka, D.R. 1976. Transepithelial transport in cell culture. *Proc. Nat. Acad. Sci. USA* **73**:1212

Mollgard, K., Malinowska, D.H., Saunders, N.R. 1976. Lack of correlation between tight junction morphology and permeability properties in developing choroid epithelium. *Nature (London)* **264**:293

Montesano, R., Friend, D.S., Perrelet, A., Orci, L. 1975. *In vivo* assembly of tight junctions in fetal liver. *J. Cell. Biol.* **67**:310

Moreno, J.H., Diamond, J.M. 1975. Cation permeation mechanisms and cation selectivity in "tight junctions" of gallbladder epithelium. *In:* Membranes: A series of Advances. G. Eisenmann, editor. Vol. 3, p. 3830. Marcel Dekker, New York

Pickett, P.B., Pitelka, D.E., Hammamoto, S.T., Misfeldt, D.S. 1975. Occluding junctions and cell behaviour in primary cultures of normal and neoplastic mammary gland cell. *J. Cell. Biol.* **66**:316

Pitelka, D.R., Hammamoto, S.T., Duafala, J.G., Nemanic, M.K. 1973. Cell contacts in the mouse mammary gland. I. Normal gland in postnatal development and the secretory cycle. *J. Cell. Biol.* **56**:797

Pricam, C., Humbert, F., Perrelet, A., Orci, L. 1974. A freeze-etch study of the tight junctions of the rat kidney tubules. *Lab. Invest.* **30**:286

Rabito, C.A., Tchao, R., Valentich, J., Leighton, J. 1978. Distribution and characteristics of the occluding junctions in a monolayer of a cell line (MDCK) derived from canine kidney. *J. Membrane Biol.* **43**:351

Reuss, L., Finn, A.L. 1975. Electrical properties of the cellular transepithelial pathway in *Necturus* gallbladder. I. Circuit analysis and steady-state effects of mucosal solution ionic substitutions. *J. Membrane Biol.* **25**:115

Reuss, L., Finn, A.L. 1976. Effects of mucosal solution hyperosmolarity on the cellular and shunt pathways of *Necturus* gallbladder (NGB) epithelium. *Biophys. J.* **16**:7*a*

Schanne, O.F., Ruíz P., Ceretti, E. 1978. Impedance measurements in biological cells. Wiley-Interscience, New York

Spring, K.R., Hope, A. 1978. Size and shape of the lateral intercellular space in a living epithelium. *Science* **200**:54

Suzuki, F., Nagano, T. 1978. Development of tight junctions in the caput epididymal epithelium of the mouse. *J. Ultrastruc. Res.* **63**:321

Tice, L.W., Carter, R.L. Cahill, M.C. 1977. Tracer and freeze fracture observations on developing tight junction in fetal rat thyroid. *Tissue Cell* **9**:395

Tice, L.W., Wollman, S.H., Carter, R.C. 1975. Changes in tight junctions of thyroid epithelium with changes in thyroid activity. *J. Cell. Biol.* **66**:657

Tisher, C.C., Yarger, W.E. 1973. Lanthanum permeability of tight junctions along the collecting duct of the rat. *Kidney Int.* **7**:35

Urakabe, S., Handler, J.D., Orloff, J. 1970. Effect of hypertonicity on permeability properties of the toad bladder. *Am. J. Physiol.* **218**:1179

Wade, J.B., Revel, J.P., DiScala, V.A. 1973. Effect of osmotic gradients on intercellular junctions of the toad bladder. *Am. J. Physiol.* **224**:407

Wedner, H.J., Diamond, J. 1969. Contributions of unstirred layer effects to apparent electrokinetic phenomena in the gallbladder. *J. Membrane Biol.* **1**:92

Whittlock, R.T., Wheeler, H.O. 1964. Coupled transport of solute and water across rabbit gallbladder epithelium. *J. Clin. Invest.* **43**:2249

Wright, E.M., Barry, P.H., Diamond, J. 1971. The mechanisms of cation permeation in rabbit gallbladder. *J. Membrane Biol.* **4**:331